Modelling radiation-effects in semiconductor lasers for use in SLHC experiments

2010 JINST 5 C12033

(http://iopscience.iop.org/1748-0221/5/12/C12033)

PUBLISHED BY IOP PUBLISHING FOR SISSA

RECEIVED: *October 30, 2010*
ACCEPTED: *November 17, 2010*
PUBLISHED: *December 15, 2010*

TOPICAL WORKSHOP ON ELECTRONICS FOR PARTICLE PHYSICS 2010,
20–24 SEPTEMBER 2010,
AACHEN, GERMANY

Modelling radiation-effects in semiconductor lasers for use in SLHC experiments

P. Stejskal,[a,b,1] **S. Détraz,**[a] **S. Papadopoulos,**[a] **I. Papakonstantinou,**[a] **C. Sigaud,**[a] **C. Soos,**[a] **S. Storey,**[a] **J. Troska**[a] **and F. Vasey**[a]

[a] *CERN,*
CH-1211 Genève 23, Switzerland
[b] *Blackett Laboratory, Imperial College,*
London SW7 2AZ, United Kingdom

E-mail: pavel.stejskal@cern.ch

ABSTRACT: Optical link components in the SLHC inner detectors are to be exposed to intense radiation fields during operation, and, hence, their qualification in terms of radiation tolerance is required. We have created a model that describes a semiconductor laser undergoing irradiation to enable the extrapolation to full lifetime total fluences from lower fluence radiation tests. This model uses a rate-equation approach with modified gain calculation that takes thermal rollover into account. The model is used to fit experimental data obtained during high-fluence (in excess of 10^{15} particles/cm^2) neutron and pion irradiation tests and evaluate its prediction capability.

KEYWORDS: Radiation damage to electronic components; Optical detector readout concepts; Radiation-hard electronics; Front-end electronics for detector readout

[1] Corresponding author.

doi:10.1088/1748-0221/5/12/C12033

Contents

2010 JINST 5 C12033

1 Introduction

High-speed optical data transmission systems have been widely deployed in the readout and control of current particle physics detectors. These optoelectronic devices operate in a very harsh radiation environment. In the past, the qualification level for optoelectronic components of a typical LHC tracker was set to a total fluence of $2 \times 10^{14}{}_{300\,\mathrm{MeV/c}}$ pions/cm^2 [1]. For the upgraded trackers, the qualification level is currently $1.5 \times 10^{15}{}_{1\,\mathrm{MeV}}$ neutrons/cm^2 [2] which imposes even more stringent demands on these systems. Their rigorous qualification and understanding in terms of performance and radiation hardness is crucial for the proper operation of the readout and control systems during the whole lifetime of the future experiments.

Radiation damage effects observed in semiconductor lasers are caused by displacement and/or ionization. Of the two, it has been found that the effects of displacement damage are much more important for the fluences and doses typical of LHC [3]. Defects known as vacancies and interstitials, which may introduce new energy levels in the band gap, can thus be created in semiconductor materials. These extra energy states act as generation-recombination centres which reduce the efficiency of band-to-band transitions.

Figure 1 illustrates a typical *L-I* curve of a laser and two most important parameters; the threshold current I_{th}, which is the drive current at which a laser starts to emit coherent light, and the output efficiency $\eta = \Delta L/\Delta I$, which is the slope of the linear part of the *L-I* curve above threshold. At higher driving currents, the *L-I* curve becomes non-linear and exhibits a so-called *thermal rollover* due to non-linear processes such as the *Auger effect* [4]. The change of the *L-I* characteristics during neutron irradiation is shown in figure 1 as well. As the total fluence increases, both the shift of the threshold current and the loss in efficiency are evident. For higher fluences, the thermal rollover is more visible.

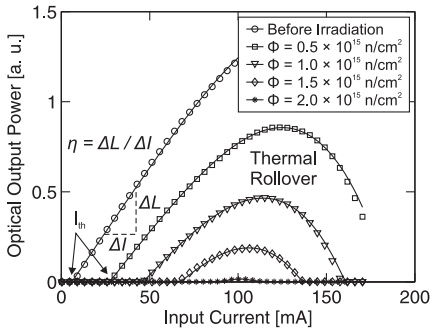

Figure 1. Set of *L-I* curves of an edge-emitting laser measured at different neutron fluences.

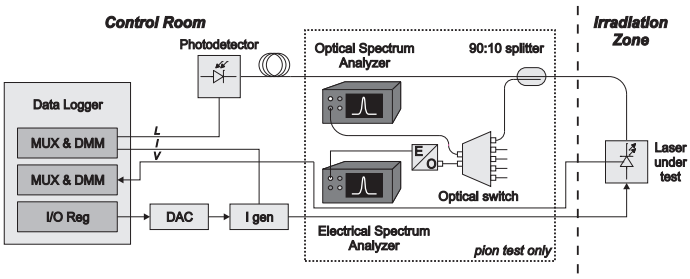

Figure 2. The measurement setup.

Lasers anneal after irradiation and can recover a significant part of the radiation-induced damage. This shows that the radiation-induced damage is flux dependent and that there would be less damage if the same fluence were accumulated over a longer irradiation period. A short-term irradiation test carried out on a timescale of tens of hours thus produces more damage in absolute terms than what would be expected in the final application where the flux is lower.

Since the usual lifetime of current particle physics detectors is counted in tens of years, the device behaviour during irradiation has to be predicted. The prediction of device behaviour during irradiation is not well established; hence an extensive testing programme for the devices in question is usually required. The testing is mainly performed in irradiation facilities by an intense and well-characterised beam of particles or ions, which serve as proxy particles for the target environment. Such testing is rather expensive and time consuming.

A complementary approach based on detailed modelling and prediction of semiconductor laser operating characteristics is described in the following sections along with a neutron and pion irradiation tests carried out at Université Catholique de Louvain (UCL) and Paul Scherrer Institut (PSI). With such a model one could significantly reduce the time spent in irradiation facilities and predict the behaviour of semiconductor lasers from low-fluence data.

2 High fluence irradiation testing

In order to evaluate new optoelectronic components in terms of their suitability for the SLHC trackers, extensive exploratory high fluence irradiation tests took place at UCL, Belgium with 20 MeV neutrons and with 300 MeV/c pions in PSI, Villigen, Switzerland. These tests aimed at evaluating the resistance of 32 prototype semiconductor lasers from eight different manufacturers to fluences in excess of 10^{15} particles/cm^2.

2.1 Irradiation setup

A schematic of the measurement setup used for both neutron and pion irradiations is shown in figure 2. The *L-I-V* characteristics of all lasers were continuously measured at approximately 20 minute intervals. The devices currently used in CMS were included for comparison to previous

2010 JINST 5 C12033

Table 1. The parameters of neutron and pion tests.

	Neutrons	Pions
Mean energy:	20 MeV	191 MeV
Irradiation time:	72 h	17 days
Annealing time:	1 month	2 weeks
Lasers irradiated:	19	13

Table 2. Irradiated devices — all devices except CMS reference are rated at 10 Gbps.

Manufacturer	# devices	Type	Wavelength [nm]	Neutron fluence [neutrons/cm^2]	Pion fluence [pions/cm^2]
1	2	Fabry-Pérot	1310	4.4×10^{15}	–
2	3+2	Fabry-Pérot	1310	4.8×10^{15}	1.2×10^{15}
2	3+2	VCSEL	850	4.7×10^{15}	1.5×10^{15}
3	3+2	VCSEL	850	4.4×10^{15}	1.5×10^{15}
4	3	Quantum dot	1310	4.8×10^{15}	–
5	3	VCSEL	1310	5.0×10^{15}	–
6	2	VCSEL	1310	–	1.6×10^{15}
7	2	VCSEL	1310	–	0.9×10^{15}
8	1	Fabry-Pérot	1310	–	1.3×10^{15}
CMS ref.	2+2	Fabry-Pérot	1310	6.3×10^{15}	1.7×10^{15}

tests. For the pion irradiation, the optical and electrical spectra were also recorded at 20 minute intervals. The parameters of the neutron and pion tests are given in table 1 and the fluences reached by all irradiated devices are summarized in table 2.

2.2 Results

The relative threshold increase versus fluence of all measured lasers is shown in figure 3(a) and figure 3(b) for neutrons and pions, respectively. The comparison between neutrons and pions for devices which underwent both tests is in figure 3(c). In terms of degradation, VCSELs prove generally to be more radiation resistant than edge-emitting lasers, while the CMS reference devices were the least radiation-hard devices. VCSELs also exhibit both the lowest relative and absolute threshold increase. Short wavelength VCSELs perform generally better than the long wavelength ones. It is obvious from the comparison plot that the scaling between neutrons and pions is different for each device type. Some lasers which stopped lasing during the irradiation recovered after a few hours. Two beam failures occurred in the neutron test during which lasers annealed some part of radiation damage which is apparent from the measured threshold curves.

3 Rate-equation model

Single-mode steady-state operation rate-equations are often used to model semiconductor laser characteristics. They are also applicable to multi-mode operation with a limited number of modes with relatively similar properties. The model describes the spontaneous- and stimulated-emission regions of laser operation and takes into account thermal rollover effects. In order to minimize the number of free parameters and to facilitate numerical solving of the equations, these are normal-

2010 JINST 5 C12033

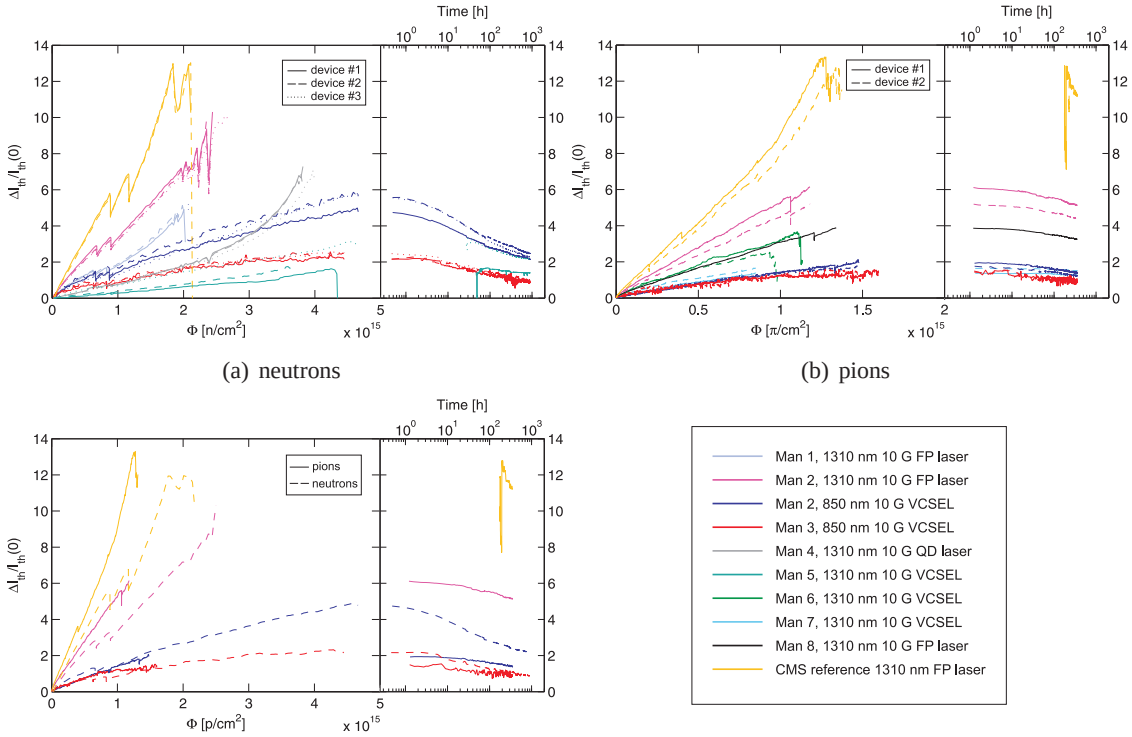

(a) neutrons (b) pions

(c) neutrons and pions (d) Legend

Figure 3. Relative threshold increase versus fluence with annealing. Typically three and two devices of the same type were irradiated in the neutron and pion test, respectively.

ized and new dimensionless quantities are introduced instead of real physical constants, which are unknown and can differ by several tens of orders of magnitude.

3.1 Theory

For a uniform electron density n in the conduction band of the active region of a semiconductor laser, the single-mode rate-equation can be written as [4, 5]:

$$\frac{\mathrm{d}n}{\mathrm{d}t} = \frac{I}{qV} - \gamma_e n - GP \tag{3.1}$$

$$\frac{\mathrm{d}P}{\mathrm{d}t} = GPV - \gamma P + R_{\mathrm{sp}}, \tag{3.2}$$

where I is the current, q the elementary charge, P the photon number within the cavity, V the volume of the active region, G is the gain per unit time and volume, R_{sp} is the spontaneous emission term and γ_e and γ are the decay rate of electron and photon, respectively. In the multi-mode case, P represents the summation over the photon numbers of individual modes, G and R_{sp} are a weighted average depending on the mode intensity.

Assuming steady state operation and expressing R_{sp} as: $R_{\mathrm{sp}} = \beta_{\mathrm{sp}}\gamma_e V n$, where β_{sp} is a fraction of photons spontaneously emitted into the lasing mode, the rate-equations (3.1) and (3.2) may be

2010 JINST 5 C12033

rewritten as:

$$J - \gamma_e n - G(n)P = 0 \tag{3.3}$$

$$P\,(G(n) - \gamma/V) + \beta_{\mathrm{sp}}\gamma_e n = 0. \tag{3.4}$$

The term $J = I/qV$, which is proportional to the drive current, can be regarded as a pumping term. To compute the equations, the explicit form of the gain G must be known [4–9]. In the simplest case, it can be expressed as $G(n) = kn$, where k is a constant.

In order to be able to solve equations (3.3) and (3.4) numerically the constants, which can differ by several tens of orders of magnitude, should be eliminated. Thus, the following dimensionless quantities are introduced:

$$N = n/n_{\mathrm{th}}, \qquad j = \frac{J}{J_{\mathrm{th}}}, \qquad p = \frac{\gamma P}{J_{\mathrm{th}} V}, \tag{3.5}$$

where the subscript 'th' denotes the quantities at threshold. The relationship between threshold current J_{th} and the electron density at threshold n_{th} is obtained from equation (3.3), where the photon number P is substituted from equation (3.4). It is customary to neglect spontaneous emission when defining J_{th} [4, 5]. Setting $\beta_{\mathrm{sp}} = 0$, we obtain: $J_{\mathrm{th}} = \gamma_e n_{\mathrm{th}}$. The electron density at threshold n_{th} is calculated from the condition $G(n_{\mathrm{th}}) = \gamma/V$. Taking these definitions into account the rate-equations may be written in a normalized form as:

$$j - N - pN = 0 \tag{3.6}$$

$$p(N-1) + \beta_{\mathrm{sp}} N = 0. \tag{3.7}$$

In order to model the thermal roll-over of semiconductor lasers, the gain term was modified to: $G(n,J) = G_0\left(n - n_0 J^l\right)$, where G_0, n_0 and l are constants. The current dependency J^l in the gain term takes into account non-linear effects such as Auger recombination and the leakage of carriers out of the active region. The modified rate-equations become:

$$j - N - p\left(\frac{N}{1-a} - \frac{a\,j^l}{1-a}\right) = 0 \tag{3.8}$$

$$p\left(\frac{N}{1-a} - \frac{a\,j^l}{1-a} - 1\right) + \beta_{\mathrm{sp}} N = 0, \tag{3.9}$$

where $a = n_0 \gamma_e J_{\mathrm{th}}^{l-1}$. Setting $l = 0$, the same *L-I* curves without a thermal rollover are obtained as from the equations (3.6) and (3.7).

3.2 Comparison with experimental data

In order to verify the applicability of the rate-equation model, the calculated operating characteristics of a semiconductor laser are compared to experimental data obtained during the high-fluence 20 MeV neutron test.

A fluence-dependent set of model parameters can be calculated using a two-step fitting of measured light-current (*L-I*) characteristics of a laser that underwent irradiation. Trends like laser threshold, quantum- and slope-efficiency are extracted and based on their behaviour the device operation during extended irradiation can be predicted. Good agreement between the calculated and measured values was reached for different technology devices in both spontaneous and stimulated emission regions of operation. Figure 4 shows a fitted data of a Mitsubishi CMS reference laser.

2010 JINST 5 C12033

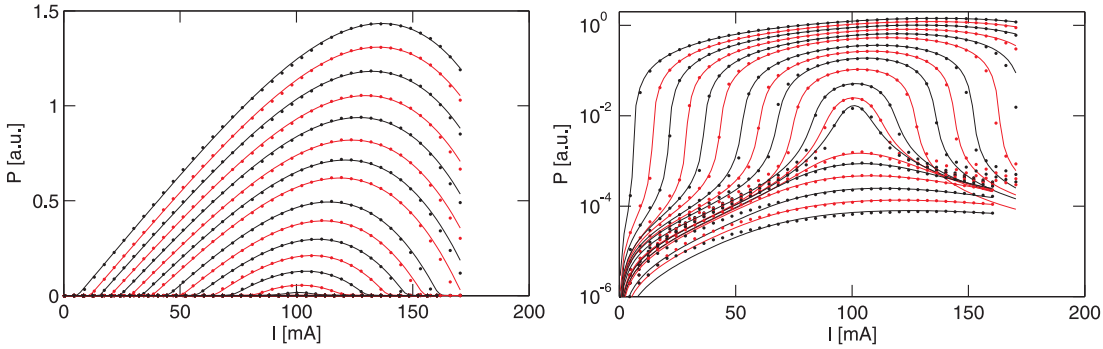

(a) linear scale (b) log. scale

Figure 4. Fitted curves for 1310 nm Mitsubishi CMS reference laser in linear and log. scale.

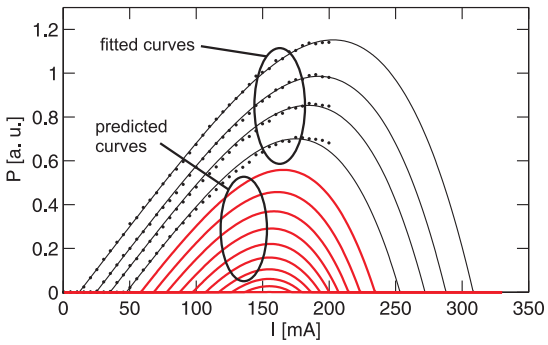

Figure 5. Fitted and predicted *L-I* curves of a 1310 nm Fabry-Pérot laser.

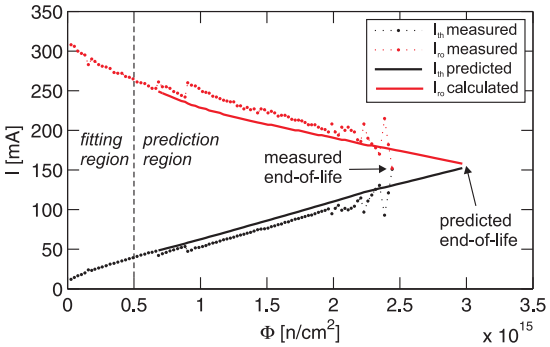

Figure 6. Measured and predicted I_{th} with calculated I_{ro} for a 1310 nm Fabry-Pérot laser.

4 Laser end-of-life prediction

Using the rate-equation model, it is possible to predict the device behaviour from low-fluence data. Data from a 1310 nm Fabry-Pérot laser in the neutron test are used as a demonstration. Fitted rate-equation model parameters from low-fluence data (below 5.0×10^{14} n/cm^2) were extrapolated and then used to predict laser *L-I* curves as depicted in figure 5. The fitted curves were extrapolated to a point where a laser stops lasing due to thermal rollover, denoted I_{ro}. The end-of-life of a laser is predicted as an intersection of I_{th} and I_{ro}. Measured values of I_{th} and I_{ro} with predicted I_{th} and calculated I_{ro} are in figure 6. This prediction currently works only for Fabry-Pérot lasers.

5 Conclusion

The proposal of using a rate-equation model to describe semiconductor laser *L-I* curves during irradiation was presented. Good agreement between the calculated and measured values was reached for all irradiated devices in both neutron and pion tests. Such a model is suitable for prediction of semiconductor laser operating characteristics during irradiation from low-fluence data. This will lead to refinement of future irradiation tests as time spent in irradiation facilities, and thus the cost, can be significantly reduced. Concerning the neutron and pion irradiation tests, only minor variations within device families were observed. In terms of annealing, lasers are able to recover a

2010 JINST 5 C12033

substantial part of the induced damage. This will be significant in the final application where the irradiation to maximum fluence takes place over the system lifetime that is typically measured in years. The measured spectral data are currently being analysed and the scaling between neutrons and pions for different device materials still needs to be evaluated.

References

[1] K. Gill et al., *Combined radiation damage, annealing, and ageing studies of InGaAsP/InP 1310 nm lasers for the CMS tracker optical links*, *Proc. SPIE* **4823** (2002) 19.

[2] L. Amaral et al., *The versatile link, a common project for super-LHC*, 2009 *JINST* **4** P12003.

[3] K. Gill et al., *Radiation damage studies of optoelectronic components for the CMS tracker optical links*, in *3rd Workshop on Electronics for LHC Experiments*, London, U.K. (1997) pp. 276–281.

[4] G.P. Agrawal and N.K. Dutta, *Semiconductor Lasers*, 2nd ed., Van Nostrand Reinhold, New York (1993), [ISBN:0-442-01102-4].

[5] R. Salathé, C. Voumard and H. Weber, *Rate equation approach for diode lasers*, *Opt. Quant. Electron.* **6** (1974) 451.

[6] H. Statz, C.L. Tang and J.M. Lavine, *Spectral Output of Semiconductor Lasers*, *J. Appl. Phys.* **35** (1964) 2581.

[7] M. Yousefi et al., *Rate Equation Model for Semiconductor Lasers With Multilongitudinal Mode Competition and Gain Dynamics*, *IEEE J. Quant. Electron.* **39** (2003) 1229.

[8] M. Bruensteiner and G.C. Papen, *Extraction of VCSEL Rate-Equation Parameters for Low-Bias System Simulation*, *IEEE Quant. Electron.* **5** (1999) 487.

[9] J. Yao et al., *Semiconductor laser dynamics beyond the rate-equation approximation*, *Optics Comm.* **119** (1995) 246.

2010 JINST 5 C12033